Localization length scales of triplet excitons in singlet fission materials

Sam L. Bayliss,[1] Karl J. Thorley,[2] John E. Anthony,[2] Hélène Bouchiat,[3] Neil C. Greenham,[1] and Alexei D. Chepelianskii[1,3,*]

[1]*Cavendish Laboratory, University of Cambridge, Cambridge, CB3 0HE, United Kingdom*

[2]*Department of Chemistry, University of Kentucky, Lexington, Kentucky 40506, USA*

[3]*LPS, Univ. Paris-Sud, CNRS, UMR 8502, F-91405, Orsay, France*

(Received 7 July 2015; revised manuscript received 1 September 2015; published 21 September 2015)

We measure the dielectric confinement length scales of triplet excitons in organic semiconductors by jointly measuring their microwave-domain electric and magnetic susceptibilities. We apply this technique to characterize triplet excitons in two singlet fission materials with distinct solid-state packing and correlate the extracted localization length scales with the role of the excitonic environment. By using the magnetic susceptibility simultaneously determined through our experiments, we compare the independently extracted dielectric and spin-spin localization length scales, highlighting the role of local anisotropy on the properties of excitonic triplet states.

DOI: 10.1103/PhysRevB.92.115432 PACS number(s): 88.40.jr, 71.35.−y, 77.84.Jd, 76.30.−v

I. INTRODUCTION

The triplet exciton, consisting of a tightly bound electron-hole pair with a total spin of one, manifests itself in many important processes relevant to carbon-based semiconductors. For example, these states are generated in the recombination of free electrons and holes in solar cells [1] or light-emitting diodes [2] which is often detrimental to optoelectronic functionality due to the inability of triplet excitons to separate into extractable carriers or radiatively recombine. The triplet exciton has therefore often been viewed as a loss pathway in organic devices. More recently however, the potential to actively utilize triplets in both photovoltaic and light-emitting devices has been realized [3–9]. Particularly important for solar-cell applications has been the process of singlet fission which enables rapid conversion of a photogenerated singlet exciton into two triplet excitons [5,6,10–13]. This provides a route to circumvent the traditional thermalization loss limit which hinders energy harvesting [14], as well new opportunities to explore and utilize optically generated triplet excitons [15–18].

While the importance of triplet excitonic states grows, their optically dark nature often makes it challenging to elucidate their physical properties; in particular, there are few techniques giving experimental access to their degree of delocalization [19]. One experimental observable which allows insight into the excitonic confinement length scale is the dielectric polarizability volume $v = \alpha/4\pi\epsilon_0$, where α is the polarizability per triplet, and ϵ_0 the vacuum permittivity. This parameter contains important information on the electrostatic confinement length scale of the triplet excitons and acts as a probe of their delocalization. For example, for singlet excitons in oligomers this quantity measures the volume of the conjugated backbone [20], while for wave functions confined to nanocrystals or fullerenes it corresponds to approximately the volume of these particles [21,22]. The polarizability is therefore an important fundamental property to access experimentally. However, in contrast to optically bright singlet excitons where electroabsorption measurements allow access to this quantity [23], for triplet excitons, this property is much more challenging to measure since selection rules forbid direct excitation of triplet excited states from the singlet ground state.

Unlike spin-zero singlet excitons however, the finite spin carried by triplet excitons offers a distinct degree of freedom to utilize in their characterization, and an unambiguous signature of their presence. This is because the dipolar interaction between electron and hole magnetic moments gives rise to an energy-level splitting between the three triplet spin sublevels, even at zero external magnetic field, governed by the zero-field-splitting Hamiltonian $\hat{H}_{zfs} = D(\hat{S}_Z^2 - \hat{\mathbf{S}}^2/3) + E(\hat{S}_X^2 - \hat{S}_Y^2)$ where D and E are the zero-field-splitting parameters, and $\hat{\mathbf{S}} = (\hat{S}_X, \hat{S}_Y, \hat{S}_Z)$ are the triplet spin operators referenced to the magnetic principal axes X, Y, Z [24]. This characteristic zero-field splitting means that triplet excitons can be readily identified through magnetic resonance, providing a direct way of observing these optically dark states [25–28]. In addition, this interaction provides an estimate of the excitonic spin-spin localization length scale since the zero-field splitting parameters are determined by the dipolar coupling between spins and hence act as a measure of their separation [24].

Here we implement a technique to extract the dielectric localization length scales of triplet excitons by jointly measuring their dielectric and spin-resonance susceptibilities which we determine through their impact on the resonance frequency of a microwave resonator. By using two prototypical singlet fission materials, TIPS-tetracene and TIPS-pentacene [29–32] (Fig. 1), which display very different solid-state environments, we correlate the observed localization length scales with the role of local anisotropy, providing a way of dielectrically characterizing dark triplet exciton states. The magnetic susceptibility simultaneously determined in our experiments allows us to compare our results to the spin interaction length scale estimated through the zero-field splitting, which acts as an independent estimate of localization due to the decoupled nature of electronic and spin degrees of freedom in organic semiconductors.

II. EXPERIMENTAL METHODS

As a direct way to measure the polarizability of triplet excitons, we implemented the contactless technique outlined in Fig. 1 which we previously applied to measure the localization

*alexei.chepelianskii@gmail.com

 ©2015 American Physical Society

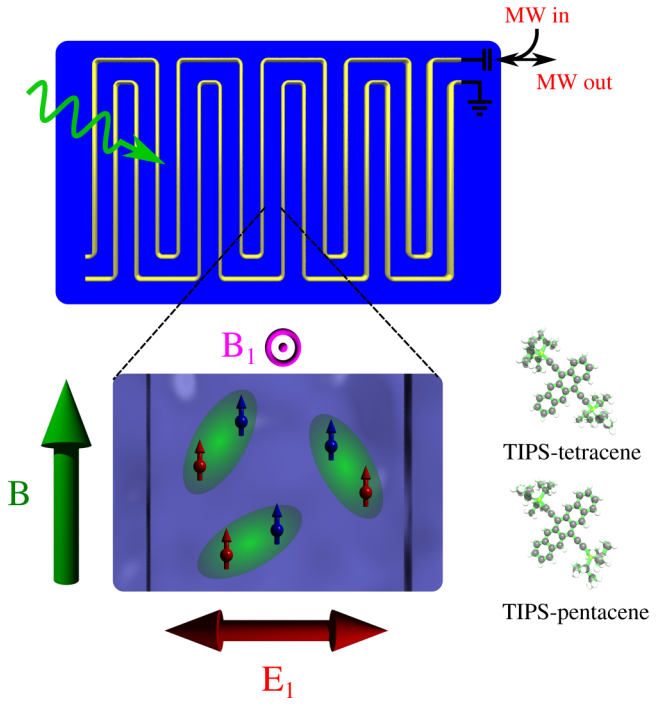


FIG. 1. (Color online) Experimental schematic for measuring the localization length scales of triplet excitons. A singlet fission material (TIPS-tetracene or TIPS-pentacene) is coupled to a microwave resonator under optical excitation, generating triplet excitons which cause a shift in the cavity resonance frequency. Tracking this frequency shift as a function of magnetic field allows extraction of their electric and magnetic susceptibilities and hence their dielectric and spin-spin localization length scales.

length scales of charges in polymer:fullerene blends [33]. Our experimental protocol uses a high-quality-factor ($Q \simeq 10^4$) microwave resonator as a sensitive means of directly measuring the triplet exciton polarizability volume through the photoinduced shifts in cavity resonance frequency. Under illumination, the generation of triplet excitons, whose charge density can be displaced within their polarizability volume v causes a net increase in the capacitance of the resonator. This shifts the resonance frequency f to lower values in proportion to the polarizability volume and total excitation number N [34]:

$$\frac{\delta f_E}{f} = -\frac{4\pi N v}{S_R \lambda_E}.$$

Here, δf_E is the frequency shift due to the increase in dielectric polarizability from photogenerated triplets, and $S_R = 2.8\ \mathrm{mm}^2$ and $\lambda_E = 19.8\ \mu\mathrm{m}$ are, respectively, the resonator surface area and the effective confinement length of the microwave electric field E_1, determined by the geometry of our cavity. To normalize by the total population N and hence extract the polarizability volume per triplet exciton, we exploit the fact that triplet excitons carry a spin of one and can therefore be counted through light-induced electron spin resonance (LESR). By applying an external magnetic field B in addition to the ac magnetic field B_1 provided by the resonator, our experiment allows us to simultaneously measure the LESR signal from triplet excitons through the shift in resonance frequency as a function of magnetic field:

$$\frac{\delta f_B}{f} = -\frac{N\chi'}{S_R \lambda_B}. \quad (1)$$

Here, χ' is the real part of the magnetic susceptibility per triplet exciton, and $\lambda_B = 5.6\ \mu\mathrm{m}$ the effective confinement length of the microwave magnetic field B_1. (We note that by tracking the resonance frequency shift, we measure the real part of the magnetic susceptibility, in contrast to typical ESR experiments where it is the imaginary part that is determined.) Taking the ratio of the dielectric to magnetic frequency shifts determined as described above allows us to extract the polarizability volume per triplet:

$$v = \left(\frac{\chi' \lambda_E}{4\pi \lambda_B}\right) \frac{\delta f_E}{\delta f_B}. \quad (2)$$

To measure these quantities experimentally, we spin-coat a layer of singlet-fission material onto a multimode Nb resonator [35–37] which we mount in an optically accessible cryostat. This provides the static field B and a stable bath temperature of $T = 2$ K, as well as allowing optical illumination with a 532 nm laser. The use of this bifilar resonator geometry is well suited for organic films since the small electromagnetic mode volume, combined with the high quality factors offered with superconducting resonators, allows for sensitive probing of the thin active layers typical of organic semiconductors. The change in resonance frequency is measured through a microwave reflectometry circuit combined with a feedback loop which allows tracking of the frequency shift as a function of illumination and magnetic field. As an unambiguous signature of triplet excitons, and due to the fact that our superconducting resonator is limited to operating at magnetic fields $B \lesssim 50$ mT, we focus here predominantly on the "half-field" transition in the LESR response [24], occurring at a magnetic field $B_{1/2} \approx hf/2g\mu_B$ where g is the electron g factor, and μ_B is the Bohr magneton (we note that we did not observe a spin-$\frac{1}{2}$ LESR from free charges in our neat films). Since this half-field transition can only occur for spin-one species it therefore acts as a direct way of identifying triplet excitons.

III. RESULTS

Figure 2(a) shows the magnetic-field-dependent frequency shift δf_B for TIPS-tetracene showing a clear LESR response characteristic of spin-one triplet excitons. The peak LESR response δf_{esr} was found to be linear with laser intensity [Fig. 2(b)] (in agreement with the kinetics found in our previous optically detected magnetic resonance (ODMR) experiments on the same material [38]). The dielectric frequency shift δf_E [Fig. 2(c)], i.e., the frequency shift under illumination at $B = 0$, also scales linearly with the laser intensity, indicating that the two frequency shifts arise from the same triplet excitons. To extract the polarizability volume from Eq. (2) the only additional parameter needed is the spin-one magnetic susceptibility χ'. We determined this quantity by numerically solving the stochastic Liouville equation for triplet excitons in the presence of microwave driving, averaging over randomly oriented molecules to determine the overall response of the film (see Appendix A for further details). Our previous ODMR

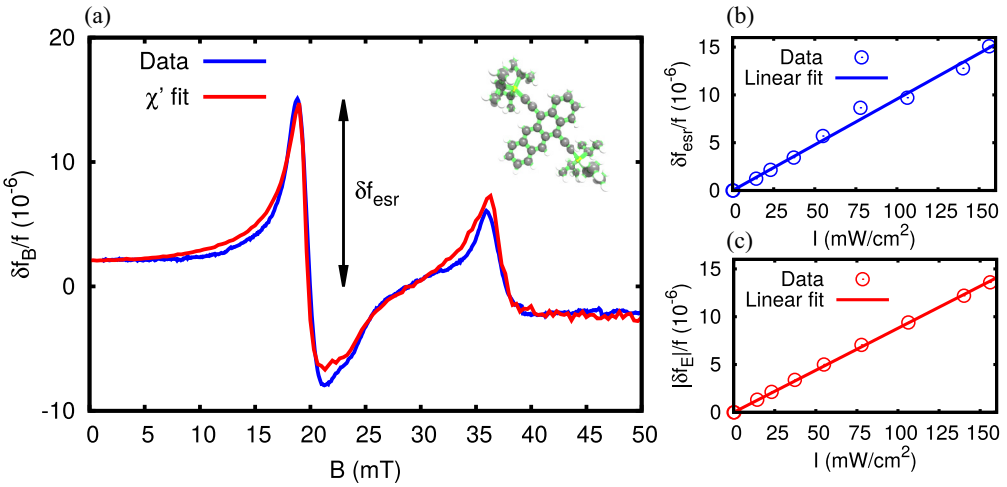


FIG. 2. (Color online) Photoinduced frequency shifts for TIPS-tetracene at 1.96 GHz. (a) Light-induced ESR response as a function of magnetic field, along with a fit to the real part of the magnetic susceptibility χ'. (b) Peak LESR signal as a function of laser intensity. (c) Frequency shift at zero magnetic field, which is determined by the dielectric polarizability, shown as a function of laser intensity.

measurements on TIPS-tetracene determined triplet zero-field-splitting parameters of $D/g\mu_B = 50\,\mathrm{mT}$ and $E \simeq 0$ which we fix in our simulations, along with the known bath temperature leaving only a line-broadening parameter which we fit to the data. The resulting fit is shown in Fig. 2(a), showing good agreement with the experimental spectrum. With χ' known, we can extract the triplet exciton polarizability volume v which we find to be $v = 15.8\ \text{Å}^3$. Rewriting $v = a^3$ in terms of an isotropic dielectric localization length a, we find $a = 2.5$ Å. We note that, due to a distribution of molecular orientations within the film, the measured polarizability is the average over the three tensorial components $\alpha = \sum_i \alpha_{ii}/3$ where $i = x,y,z$ are the principal axes. In the case of maximal anisotropy, where only one component contributes, the localization length determined from this component will therefore be $a' = 3^{1/3}a \simeq 1.4a$, which provides an upper bound for the most delocalized length scale. The triplet zero-field-splitting parameters, which measure the strength of the spin dipole-dipole interaction between electron and hole and hence their spin-spin localization length, provide an independent measure of triplet exciton localization since the orbital and spin degrees of freedom are effectively decoupled in organic materials. Using the value of D for TIPS-tetracene, the spin-spin localization length is $r_{ss} = 3.8$ Å which is reasonably close to the independently measured dielectric localization length a. We note that these estimates indicate a highly localized triplet state (Fig. 4 displays representative molecular and crystal length scales for comparison), consistent with the weak intermolecular coupling suggested by the TIPS-tetracene crystal packing [Fig. 4(a)] [38], and other estimates of triplet localization in organic semiconductors [19,39,40].

To investigate the influence of molecular size and packing on the polarizability and spin-spin-localization length scales we carried out experiments using the molecule

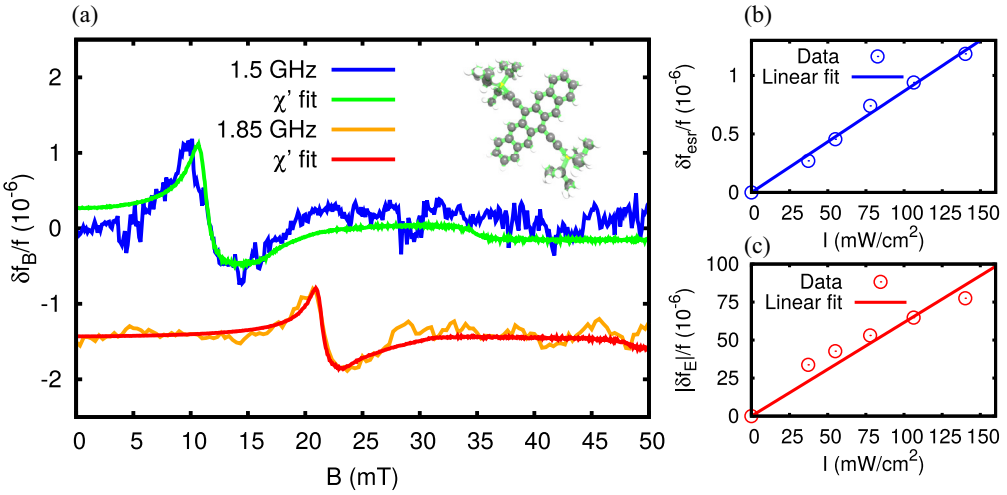


FIG. 3. (Color online) Photoinduced frequency shifts for TIPS-pentacene. (a) LESR response for two different resonator harmonics and corresponding fits to the magnetic susceptibility χ'. (b) Peak LESR signal as a function of laser intensity. (c) Dielectric frequency shift at zero magnetic field as a function of laser intensity.

TIPS-pentacene [31,41,42] which has one more aromatic ring than TIPS-tetracene. Since, to our knowledge, the zero-field splitting parameters of TIPS-pentacene have not been determined, we measured the magnetic susceptibility response at two different resonator harmonics to provide a consistent determination of these quantities [Fig. 3(a)], yielding $D/g\mu_B = 41$ mT, $E/g\mu_B = 6$ mT. As with TIPS-tetracene, we find $\delta f_{\rm esr}$ and δf_E scale approximately linearly with the laser intensity [Figs. 3(b) and 3(c)] but yield a larger polarizability volume of $v = 1100$ Å^3 corresponding to an isotropic dielectric localization length scale of $a = 10.3$ Å. From the zero-field-splitting parameter D, we find $r_{\rm ss} = 4.1$ Å.

IV. DISCUSSION

As expected based on an increase in molecular size in going from TIPS-tetracene to TIPS-pentacene, both spin-spin- and dielectric-localization length scales increase; however, the increase in the dielectric confinement length is much more striking than for the spin-spin case. From a simple perspective based on the modest increase in molecular size, one might expect a relatively modest increase in the polarizability volume between the two molecules with four- and five-membered acene backbones. However, this neglects the role that anisotropy, which can be influenced by both the molecular and solid-state properties, plays in determining these parameters.

To construct an intuitive picture for the influence of anisotropy on the dielectric and spin-spin-localization length scales, we take an anisotropic harmonic potential $V(\mathbf{r}) = \frac{1}{2}m(\omega_x^2x^2 + \omega_y^2y^2 + \omega_z^2z^2)$ to represent the confining environment, where m is the effective mass and $\omega_x,\omega_y,\omega_z$ are the oscillator frequencies. The polarizability volume can be derived for this anisotropic environment by considering the displacement of charge caused by an electric field which we average over random orientations to account for the distribution of molecular orientations within the film. This yields $v = \frac{e^2}{12m\pi\epsilon_0}(\omega_x^{-2} + \omega_y^{-2} + \omega_z^{-2})$, where e is the electronic charge. In the presence of a strong anisotropy direction, for example $\omega_x \ll \omega_y,\omega_z$, the polarizability will therefore be dominated by the most weakly confined direction i.e., $v \sim \omega_x^{-2}$, giving rise to an enhancement of the extracted localization length scale, as we observe between TIPS-tetracene and TIPS-pentacene.

The approximate scaling of the spin-spin interaction length scale on the different anisotropic dimensions can also be derived using this framework by considering the expectation of the zero-field-splitting Hamiltonian over a suitable wave function. Written in a form which more explicitly reflects the dipolar nature of this interaction [24], and the associated interaction length scale, we have

$$\hat{H}_{zfs} = \beta\left(\frac{\hat{\mathbf{s}}_\mathbf{1}\cdot\hat{\mathbf{s}}_\mathbf{2}}{r^3} - 3\frac{(\hat{\mathbf{s}}_\mathbf{1}\cdot\mathbf{r})(\hat{\mathbf{s}}_\mathbf{2}\cdot\mathbf{r})}{r^5}\right), \tag{3}$$

where $\beta = \frac{\mu_0}{4\pi}(g\mu_B\hbar)^2$, $\hat{\mathbf{s}}_\mathbf{1}$ and $\hat{\mathbf{s}}_\mathbf{2}$ are the spin operators for the two electrons, and $\mathbf{r} = \mathbf{r_1} - \mathbf{r_2}$ is the vector between them with $r = |\mathbf{r}|$. For triplet states with a symmetric spin wave function, the orbital wave function must be antisymmetric, which in a two-state basis formed of single-particle wave functions ϕ_a,ϕ_b becomes

$$\Phi(\mathbf{r}_1,\mathbf{r}_2) = \frac{1}{\sqrt{2}}\begin{vmatrix}\phi_a(\mathbf{r_1}) & \phi_b(\mathbf{r_1})\\ \phi_a(\mathbf{r_2}) & \phi_b(\mathbf{r_2})\end{vmatrix}.$$

(We note that the exclusion principle enforced by this Slater determinant removes any singular behavior in the expectation value of the dipole-dipole interaction associated with the limit $r \to 0$.) To proceed analytically, we take ϕ_a as the ground-state wave function $\phi_a(\mathbf{r}) = \prod_i \phi_0(r_i)$ where $\phi_0(r_i)$ are the single-particle harmonic oscillator ground-state wave functions in the directions $r_i = x,y,z$, and ϕ_b as a singly excited state $\phi_b(\mathbf{r}) = \phi_1(r_j)\prod_{i\neq j}\phi_0(r_i)$ where $\phi_1(r_j)$ is the first excited harmonic oscillator wave function along the direction r_j. With these wave functions, the dependence of the dipole-dipole interaction on the anisotropic confinement can be found by calculating the expectation $\langle\hat{H}_{zfs}\rangle = \langle\Phi|\hat{H}_{zfs}|\Phi\rangle$. Unlike the polarizability volume, we find that the zero-field splitting is no longer dominated by only one confinement direction and exhibits a weaker dependence on the anisotropy. For the uniaxial case $\omega_y = \omega_z = \omega$ with a single-particle excitation along z, i.e., $\phi_b(\mathbf{r}) = \phi_0(x)\phi_0(y)\phi_1(z)$, we are able to obtain an analytic expression for the D parameter (see Appendix B).

The different scalings of the polarizability volume and D parameter in this model are shown in Fig. 4(c) which plots the normalized values v/v_0, D_0/D, and their ratio vD/v_0D_0 as a function of the anisotropy ω/ω_x, where v_0 and D_0 are the corresponding values for $\omega_x = \omega_y = \omega_z = \omega$. Since v and βD^{-1} represent polarizability and spin-spin-interaction volumes, respectively, this plot highlights the different scaling of these two parameters with anisotropy. The stronger dependence of the polarizability volume on anisotropy compared to the zero-field splitting D is apparent, clearly reflected in the ratio vD/v_0D_0, which for the same dependence on anisotropy should be independent of ω/ω_x, but grows strongly with this anisotropy ratio. While our estimates will in general depend on the precise exciton wave functions, they highlight the different way that anisotropy is reflected in the polarizability and spin-spin length scales, borne out through the values measured in the two different materials systems.

Turning to the physical origin of this anisotropy, we note that this can have contributions from both the intramolecular environment—for example, the breaking of molecular symmetry by the TIPS groups in TIPS-tetracene, but not in TIPS-pentacene—as well as contributions from the intermolecular environment, where the distinct crystal packing in the two materials suggests itself as a contributing factor. For TIPS-tetracene, the crystal packing [41,43] [Fig. 4(a)] indicates a modest π-π interaction due to the distinct orientations of neighboring molecules (also pointed to by the similarity between absorption spectra in solution and solid state). For TIPS-pentacene however, the face-to-face stacking shown in Fig. 4(b) indicates a significantly more anisotropic environment [41,44], and a greater influence of intermolecular interactions between neighboring molecules [42,44] (also pointed to by the significant difference between solution and film absorption spectra [31]). We note that anisotropy has been shown to play an important role in triplet exciton diffusion in molecular semiconductors, with the experimental

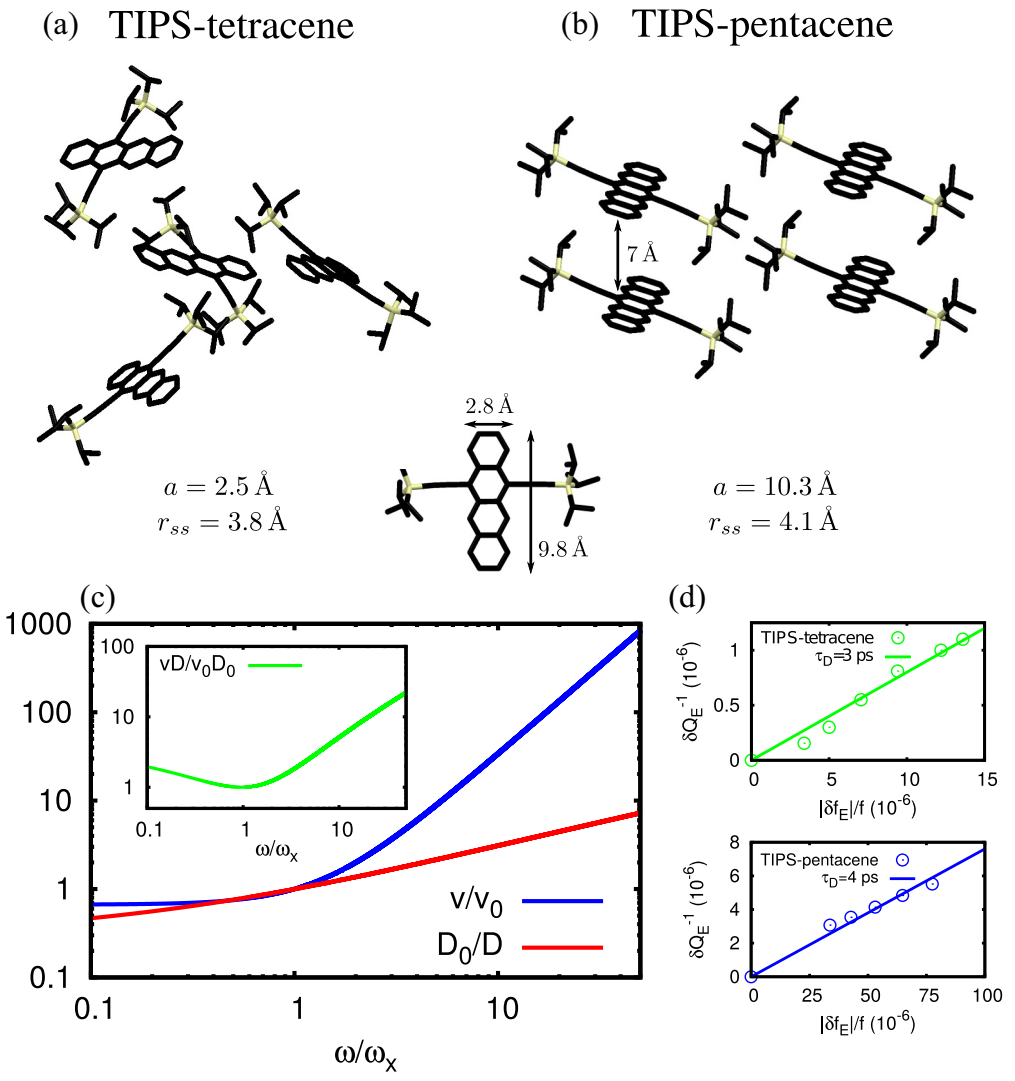


FIG. 4. (Color online) (a), (b) Molecular packing of the two materials, typical molecular and crystal length scales, and summary of the measured isotropic dielectric confinement length scales a and spin-confinement lengths r_{ss}. For (a) TIPS-tetracene there are four rotationally inequivalent molecules in the unit cell while for (b) TIPS-pentacene, each molecule is rotationally equivalent. (c) Scalings with anisotropy: normalized polarizability volume v/v_0 and inverse zero-field-splitting parameter D_0/D (which represents the normalized spin-spin interaction volume), as well as their ratio, calculated within the model described in the main text as a function of the anisotropy ω/ω_x. (d) Imaginary and real parts of the dielectric frequency shift used to determine the Debye response times. The different points correspond to different light intensities.

characterization typically relying on radiative triplet-triplet annihilation to track energy migration [15,45,46]. By using the polarizability, the results presented here open up a different way of probing anisotropy without the requirement for an emissive recombination channel.

Finally, in addition to estimating the dielectric localization length scales, our experiments also allow us to estimate the characteristic dielectric relaxation time associated with the triplets τ_D by comparing the real and imaginary parts of the dielectric susceptibility. This parameter, which reflects how fast the triplet excitons can respond to the ac electric field E_1, is accessible through our experiments by comparing the frequency shift δf_E and the change in inverse quality factor of the resonator δQ_E^{-1} at zero magnetic field, shown in Fig. 4(d) for different laser intensities. Taking a Debye response (corresponding to exponential relaxation) of $\alpha(\omega) = \alpha_0/(1+\omega\tau_D)$, with $\omega = 2\pi f$, the dielectric relaxation time is given by $\tau_D = \frac{1}{\omega}\frac{\frac{1}{2}\delta Q_E^{-1}}{(|\delta f_E|/f)}$. For both materials we find a similar response time of $\tau_D = 3$ to 4 ps, this relatively fast response reflecting the localized nature of the excitonic triplet states. Furthermore, with the known magnetic susceptibility, and film thicknesses measured through atomic force microscopy to be $W \simeq 500$ nm for TIPS-tetracene and $W \simeq 225$ nm for TIPS-pentacene, Eq. (1) allows us to estimate the triplet density n in our experiments. At peak illumination, we find $n = 3.3 \times 10^{24}$ m^{-3} for TIPS-tetracene and $n = 4.5 \times 10^{23}$ m^{-3} for TIPS-pentacene, giving average triplet separations of $n^{-1/3} = 7$ nm and 13 nm. This corresponds to roughly one triplet per 300 molecules for TIPS-tetracene and one triplet per 2300 molecules for TIPS-pentacene, based on

the molecular density determined from the crystal unit cells (Fig. 4).

V. CONCLUSION

To summarize, we implemented an experimental technique to extract the dielectric localization length scale of triplet excitons which we applied to two model singlet fission materials. Using this technique, we compared the dielectric localization length scale, which characterizes the distance over which the excitonic charge density is confined, with the independently estimated spin-spin interaction length scale which characterizes the distance over which electron and hole interact through the magnetic dipolar interaction. These results highlight the localized nature of triplet excitons in organic semiconductor materials and the role of anisotropy in the local excitonic environment. Our experiments demonstrate the utility of dielectric and magnetic susceptibility measurements to investigate the properties of excitonic triplet states.

ACKNOWLEDGMENTS

We acknowledge support from the Engineering and Physical Sciences Research Council (Grant No. EP/G060738/1), the Royal Society International Exchange Scheme and Investissements d'Avenir du LabEx PALM (ANR-10-LABX-0039-PALM). A.D.C. acknowledges support from and St. Catharine's College, Cambridge. S.L.B. is grateful for support from the EPSRC Supergen SuperSolar Project, and Magdalene College, Cambridge. J.E.A. and K.J.T. thank the National Science Foundation (CMMI-1255494) for support of organic semiconductor synthesis. We thank N. Kirova and A. Musser for fruitful discussions and L. Yang and L. Weiss for experimental assistance. The data underlying this paper are available at www.repository.cam.ac.uk/handle/1810/250509.

APPENDIX A: MAGNETIC SUSCEPTIBILITY

To calculate the magnetic susceptibility χ' we solve the equation of motion for the triplet exciton density matrix $\hat{\rho}$ under microwave irradiation:

$$\partial_t \hat{\rho}_{nm} = -\frac{i}{\hbar}[\hat{H}_0 + \hat{H}_1(t), \hat{\rho}]_{nm} - \gamma\left(\hat{\rho}_{nm} - \hat{\rho}^{eq}_{nm}\right). \quad \text{(A1)}$$

Here, $\hat{H}_0 = \hat{H}_Z + \hat{H}_{zfs}$ is the static spin Hamiltonian consisting of the Zeeman interaction, $\hat{H}_Z = g\mu_B \mathbf{B}\cdot\hat{\mathbf{S}}$ where $\mathbf{B}$ is the external magnetic field, and the zero-field-splitting Hamiltonian $\hat{H}_{zfs}$. $\hat{H}_1(t) = g\mu_B \mathbf{B_1}(t)\cdot\hat{\mathbf{S}}$ is the ac spin Hamiltonian with microwave magnetic field $\mathbf{B_1}(t)$, γ the decay term which acts as a line-broadening parameter, and $\hat{\rho}^{eq}$ is the thermal equilibrium density matrix. Working in the eigenbasis of the static Hamiltonian such that $\hat{H}_{0,nm} = \hbar\omega_{nm}\delta_{nm}$, where ω_{nn} are the eigenvalues of $\hat{H}_0$, the susceptibility is found by first performing a perturbative expansion of $\hat{\rho}$ in powers of $\hat{H}_1(t)$ and solving for the first-order contribution [47]:

$$\rho^{(1)}_{nm} = -\frac{g\mu_B}{\hbar}\left(\rho^{eq}_{mm} - \rho^{eq}_{nn}\right)\sum_{\omega}\frac{(\mathbf{S}\cdot\mathbf{B_1}(\omega))_{nm}e^{-i\omega t}}{(\omega_{nm}-\omega)-i\gamma}, \quad \text{(A2)}$$

where we introduced the Fourier decomposition of $\mathbf{B_1}(t) = \sum_\omega \mathbf{B_1}(\omega)e^{-i\omega t}$ where ω is the microwave frequency. The susceptibility is found from the induced magnetization $\mathbf{m}(\omega) = g\mu_B \mathrm{Tr}(\rho^{(1)}\mathbf{S}) = \chi^{(1)}\mathbf{B_1}(\omega)/\mu_0$, which yields

$$\chi^{(1)} = -\frac{\mu_0(g\mu_B)^2}{\hbar}\sum_{nm}\left(\rho^{eq}_{mm} - \rho^{eq}_{nn}\right)\frac{(\mathbf{S}\cdot\hat{\mathbf{n}})_{mn}(\mathbf{S}\cdot\hat{\mathbf{n}})_{nm}}{(\omega_{nm}-\omega)-i\gamma}, \quad \text{(A3)}$$

where $\hat{\mathbf{n}}$ is the unit vector in the direction of the ac magnetic field $\mathbf{B_1}$. This expression gives us the susceptibility for a single triplet with its zero-field-splitting tensor at a fixed orientation with respect the magnetic field. To find the response of the film, we average over molecular orientations to obtain the total susceptibility, whose real part χ' determines the LESR frequency shift δf_B.

APPENDIX B: EXPECTATION OF THE ZERO-FIELD-SPLITTING HAMILTONIAN

To extract the D parameter within the model presented in the main text, we rewrite the expectation of the zero-field-splitting Hamiltonian [Eq. (3)] in terms of relative, and center-of-mass coordinates: $\mathbf{r} = \mathbf{r}_1 - \mathbf{r}_2$ and $\mathbf{R} = (\mathbf{r}_1 + \mathbf{r}_2)/2$:

$$\langle\hat{H}_{zfs}\rangle = \langle\Phi_R(\mathbf{R})|\Phi_R(\mathbf{R})\rangle\langle\Phi_r(\mathbf{r})|\hat{H}_{zfs}(\mathbf{r})|\Phi_r(\mathbf{r})\rangle,$$

where $|\Phi(\mathbf{r}_1,\mathbf{r}_2)\rangle = |\Phi_R(\mathbf{R})\rangle|\Phi_r(\mathbf{r})\rangle$. This separates the calculation into an integration over center-of-mass coordinates, and the expectation of $\hat{H}_{zfs}$ over relative coordinates which can both be performed analytically. The D parameter is recovered by moving from the representation of $\hat{H}_{zfs}$ in the two-electron basis, with spin operators $\hat{\mathbf{s}}_1$ and $\hat{\mathbf{s}}_2$ [Eq. (3)], to the representation in the triplet basis, with spin operator $\hat{\mathbf{S}}$ [$\hat{H}_{zfs} = D(\hat{S}_z^2 - \hat{\mathbf{S}}^2/3) + E(\hat{S}_x^2 - \hat{S}_y^2)$], which can be achieved by using the relation $\hat{s}_{1,i}\hat{s}_{2,i} = \frac{1}{2}(\hat{S}_i^2 - \frac{1}{4}\hat{\mathbf{S}}^2)$.

[1] A. Rao, P. C. Y. Chow, S. Gélinas, C. W. Schlenker, C.-Z. Li, H.-L. Yip, A. K.-Y. Jen, D. S. Ginger, and R. H. Friend, Nature (London) **500**, 435 (2013).
[2] A. P. Monkman, ISRN Mater. Sci. **2013**, 19 (2013).
[3] T. N. Singh-Rachford and F. N. Castellano, Coord. Chem. Rev. **254**, 2560 (2010).
[4] H. Uoyama, K. Goushi, K. Shizu, H. Nomura, and C. Adachi, Nature (London) **492**, 234 (2012).
[5] M. B. Smith and J. Michl, Chem. Rev. (Washington, DC, U. S.) **110**, 6891 (2010).
[6] M. B. Smith and J. Michl, Annu. Rev. Phys. Chem. **64**, 361 (2013).
[7] D. N. Congreve, J. Lee, N. J. Thompson, E. Hontz, S. R. Yost, P. D. Reusswig, M. E. Bahlke, S. Reineke, T. Van Voorhis, and M. A. Baldo, Science **340**, 334 (2013).
[8] P. J. Jadhav, P. R. Brown, N. Thompson, B. Wunsch, A. Mohanty, S. R. Yost, E. Hontz, T. Van Voorhis, M. G. Bawendi, V. Bulović, and M. A. Baldo, Adv. Mater. **24**, 6169 (2012).
[9] B. Ehrler, M. W. B. Wilson, A. Rao, R. H. Friend, and N. C. Greenham, Nano Lett. **12**, 1053 (2012).

[10] S. T. Roberts, R. E. McAnally, J. N. Mastron, D. H. Webber, M. T. Whited, R. L. Brutchey, M. E. Thompson, and S. E. Bradforth, J. Am. Chem. Soc. **134**, 6388 (2012).
[11] W.-L. Chan, J. R. Tritsch, and X.-Y. Zhu, J. Am. Chem. Soc. **134**, 18295 (2012).
[12] J. C. Johnson, A. J. Nozik, and J. Michl, J. Am. Chem. Soc. **132**, 16302 (2010).
[13] M. W. B. Wilson, A. Rao, J. Clark, R. S. S. Kumar, D. Brida, G. Cerullo, and R. H. Friend, J. Am. Chem. Soc. **133**, 11830 (2011).
[14] M. C. Hanna and A. J. Nozik, J. Appl. Phys. **100**, 074510 (2006).
[15] P. Irkhin and I. Biaggio, Phys. Rev. Lett. **107**, 017402 (2011).
[16] J. J. Burdett and C. J. Bardeen, J. Am. Chem. Soc. **134**, 8597 (2012).
[17] N. J. Thompson, M. W. B. Wilson, D. N. Congreve, P. R. Brown, J. M. Scherer, T. S. Bischof, M. Wu, N. Geva, M. Welborn, T. Van Voorhis, V. Bulović, M. G. Bawendi, and M. A. Baldo, Nat. Mater. **13**, 1039 (2014).
[18] M. Tabachnyk, B. Ehrler, S. Gélinas, M. L. Böhm, B. J. Walker, K. P. Musselman, N. C. Greenham, R. H. Friend, and A. Rao, Nat. Mater. **13**, 1033 (2014).
[19] G. H. Gelinck, J. J. Piet, and J. M. Warman, Synth. Met. **101**, 553 (1999).
[20] G. H. Gelinck, J. J. Piet, B. R. Wegewijs, K. Müllen, J. Wildeman, G. Hadziioannou, and J. M. Warman, Phys. Rev. B **62**, 1489 (2000).
[21] G. K. Gueorguiev, J. M. Pacheco, and D. Tománek, Phys. Rev. Lett. **92**, 215501 (2004).
[22] S. A. Empedocles and M. G. Bawendi, Science **278**, 2114 (1997).
[23] A. Horvath, H. Bassler, and G. Weiser, Phys. Status Solidi B **173**, 755 (1992).
[24] J. A. Weil and J. R. Bolton, in *Electron Paramagnetic Resonance* (Wiley, New Jersey, 2007), Chap. 6, pp. 162–187.
[25] J. Shinar, Laser Photon. Rev. **6**, 767 (2012).
[26] W. J. Baker, D. R. McCamey, K. J. van Schooten, J. M. Lupton, and C. Boehme, Phys. Rev. B **84**, 165205 (2011).
[27] L. Hachani, A. Benfredj, S. Romdhane, M. Mejatty, J. L. Monge, and H. Bouchriha, Phys. Rev. B **77**, 035212 (2008).
[28] M. Bennati, A. Grupp, M. Mehring, and P. Bäuerle, J. Phys. Chem. **100**, 2849 (1996).
[29] TIPS-tetracene is bis(triisopropylsilylethynyl)tetracene, TIPS-pentacene is bis(triisopropylsilylethynyl)pentacene. Both materials were prepared from chloroform solution.
[30] H. L. Stern, A. J. Musser, S. Gelinas, P. Parkinson, L. M. Herz, M. J. Bruzek, J. Anthony, R. H. Friend, and B. J. Walker, Proc. Natl. Acad. Sci. USA **112**, 7656 (2015).
[31] B. J. Walker, A. J. Musser, D. Beljonne, and R. H. Friend, Nat. Chem. **5**, 1019 (2013).
[32] A. J. Musser, M. Liebel, C. Schnedermann, T. Wende, T. B. Kehoe, A. Rao, and P. Kukura, Nat. Phys. **11**, 352 (2015).
[33] A. D. Chepelianskii, J. Wang, and R. H. Friend, Phys. Rev. Lett. **112**, 126802 (2014).
[34] L. D. Landau and E. M. Lifshitz, in *Electrodynamics of Continuous Media* (Pergamon Press, New Jersey, 1984), Chap. 10, pp. 310–313.
[35] B. Dassonneville, M. Ferrier, S. Guéron, and H. Bouchiat, Phys. Rev. Lett. **110**, 217001 (2013).
[36] B. Reulet, M. Ramin, H. Bouchiat, and D. Mailly, Phys. Rev. Lett. **75**, 124 (1995).
[37] A. D. Chepelianskii, F. Chiodi, M. Ferrier, S. Gúron, E. Rouviere, and H. Bouchiat, Appl. Phys. Lett. **96**, 052118 (2010).
[38] S. L. Bayliss, A. D. Chepelianskii, A. Sepe, B. J. Walker, B. Ehrler, M. J. Bruzek, J. E. Anthony, and N. C. Greenham, Phys. Rev. Lett. **112**, 238701 (2014).
[39] F. C. Grozema, R. Telesca, H. T. Jonkman, L. D. A. Siebbeles, and J. G. Snijders, J. Chem. Phys. **115**, 10014 (2001).
[40] S. Sharifzadeh, P. Darancet, L. Kronik, and J. B. Neaton, J. Phys. Chem. Lett. **4**, 2197 (2013).
[41] J. E. Anthony, J. S. Brooks, D. L. Eaton, and S. R. Parkin, J. Am. Chem. Soc. **123**, 9482 (2001).
[42] C. D. Sheraw, T. N. Jackson, D. L. Eaton, and J. E. Anthony, Adv. Mater. **15**, 2009 (2003).
[43] J. E. Anthony, J. S. Brooks, D. L. Eaton, and S. R. Parkin, CCDC 172476: Experimental Crystal Structure Determination, 2001 doi:10.5517/cc5sgr4.
[44] J. E. Anthony, D. L. Eaton, and S. R. Parkin, Org. Lett. **4**, 15 (2002).
[45] P. Sibani and J. B. Pedersen, Phys. Rev. B **26**, 2584 (1982).
[46] V. Ern, Phys. Rev. Lett. **22**, 343 (1969).
[47] W. R. Boyd, in *Nonlinear Optics*, 2nd ed. (Academic Press, San Diego, 2003), Chap. 3, pp. 151–156.